COMPARISON BETWEEN A CENTERED AND A HIGH RESOLUTION UPWIND SCHEMES IN THE SOLUTION OF AEROSPACE PROBLEMS USING UNSTRUCTURED STRATEGY

Edisson Sávio de Góes Maciel
Rua Demócrito Cavalcanti, 152 - Afogados
Recife – PE – Brazil - CEP 50750-080
e-mail: edissonsavio@yahoo.com.br

Abstract. *The present work performs a comparison between a centered numerical scheme and a high resolution upwind scheme. The Jameson and Mavriplis algorithm, on the context of a centered spatial discretization and second order spatial accuracy, and the Frink, Parikh and Pirzadeh algorithm, on the context of upwind spatial discretization, using a flux difference splitting formulation and first order spatial accuracy, both explicit in time, are studied. The Jameson and Mavriplis algorithm uses an artificial dissipation operator to guarantee numerical stability. The Euler equations in conservative form, using a finite volume formulation and an unstructured spatial discretization of the flow equations, in two-dimensions, are solved. The transonic flow around a NACA 0012 airfoil and the supersonic flow around a simplified configuration of VLS are physical problems studied in this work. Both problems are studied in steady state regime and a zero angle of attack is adopted. The time integration uses a Runge-Kutta time stepping method of five stages and second order of accuracy. Results have shown good agreement between the algorithms with better solution quality characteristics and convergence acceleration properties to the Jameson and Mavriplis scheme.*

Keywords*: Unstructured algorithms, Centered and high resolution upwind algorithms, Euler equations, Finite volume method, Aerospace problems.*

1. Introduction

The necessity of practical tests in several aerodynamics components of airplanes and aerospace vehicles during the project phase, in aeronautical and aerospace industries, is limited by the expensive cost due to the construction of scaled models and to perform tests in wind tunnels. Other main difficulties are related to the high number of experimental tests required during the optimization phase of these models. The development of computer technology, allowing the existence of high speed processors and high store capability, has boomed Computational Fluid Dynamics, CFD, towards to a meaningful role in several industry areas. Such areas require low cost levels during the experimental development and high performance of their products.

In this work, the Jameson and Mavriplis (1986) and the Frink, Parikh and Pirzadeh (1991) explicit schemes, the last one using the flux difference splitting of Roe (1981), are compared using a finite volume formulation, based on a cell centered data base. The Jameson and Mavriplis (1986) scheme is really the most employed algorithm in terms of unstructured discretization of the fluid movement equations (Mavriplis and Jameson, 1987, Batina, 1990, Arnone, Liou and Povinelli, 1991, Long, Khan and Sharp, 1991, Swanson and Radespiel, 1991, and Hooker, Batina and Williams, 1992). The Frink, Parikh and Pirzadeh (1991) is a high resolution upwind scheme and presents good robustness properties (Frink, 1992, and Liou, Baum and Löhner, 1994). This comparison intends to emphasize important aspects of these algorithms in relation to: computational performance and some aspects of solution quality The physical problems of the transonic flow around a NACA 0012 airfoil and the supersonic flow around a simplified version of VLS configuration are studied using an unstructured discretization of the flow equations.

An unstructured discretization of the spatial domain is often recommended to complex configurations due to the facility and efficiency of domain discretization (Jameson and Mavriplis, 1986, Mavriplis, 1990, Batina, 1990, and Pirzadeh, 1991). However, the unstructured generation question will not be studied in this work. The main objective of this work is to highlight the numerical features of the Jameson and Mavriplis (1986) and the Frink, Parikh and Pirzadeh (1991) schemes in the solution of the Euler equations, regardless of the method used for grid generation.

2. Euler equations

The fluid movement is governed by the Euler equations, which express the mass, momentum and energy conservations of an inviscid, heat non-conductor and compressible mean, in the absence of external forces. In integral and conservative forms, these equations can be represented by:

$$\partial/\partial t \int_V Q dV + \int_S \left(E_e n_x + F_e n_y\right) dS = 0 \,, \tag{1}$$

where Q is written to a Cartesian system, V is the volume of a cell, n_x and n_y are normal unity vectors in relation to each flux face, S is the flux area and E_e and F_e represent the convective flux vector components. Q, E_e and F_e are represented by:

$$Q = \begin{Bmatrix} \rho \\ \rho u \\ \rho v \\ e \end{Bmatrix}, \quad E_e = \begin{Bmatrix} \rho u \\ \rho u^2 + p \\ \rho uv \\ (e + p)u \end{Bmatrix} \text{ and } F_e = \begin{Bmatrix} \rho v \\ \rho uv \\ \rho v^2 + p \\ (e + p)v \end{Bmatrix}, \tag{2}$$

where ρ is the fluid density; u and v are Cartesian components of the velocity vector in the x and y directions, respectively; e is the total energy per unity volume; and p is the static pressure. Expressions to the flux area S and to the volumes V are available in Maciel and Azevedo (2001) and in Maciel (2002).

The nondimensionalization applied to the Euler equations for all problems was accomplished in relation to the freestream density, ρ_∞, and freestream speed of sound, a_∞. The matrix system of the Euler equations is closed using the perfect gas state equation $p = (\gamma - 1)\left[e - 0.5\rho(u^2 + v^2)\right]$ with γ being the ratio of specific heats. The total enthalpy is determined by $h = \left[\gamma/(\gamma - 1)\right](p/\rho) + 0.5(u^2 + v^2)$.

3. Jameson and Mavriplis (1986) algorithm

The Euler equations in conservative and integral forms, according to a finite volume formulation, can be written, on a context of unstructured spatial discretization (Jameson, Schmidt and Turkel, 1981, Jameson and Mavriplis, 1986, and Maciel and Azevedo, 2001), as:

$$d(V_i Q_i)/dt + C(Q_i) = 0, \tag{3}$$

where $C(Q_i) = \sum_{k=1}^{3}\left[E_e(Q_{i,k})\Delta y_{i,k} - F_e(Q_{i,k})\Delta x_{i,k}\right]$ is the discrete approximation to the flux integral of Eq. (1). In this work, it was adopted that:

$$Q_{i,k} = 0.5(Q_i + Q_k), \quad \Delta y_{i,k} = y_{n2} - y_{n1} \text{ and } \Delta x_{i,k} = x_{n2} - x_{n1}, \tag{4}$$

with "*i*" indicating a given mesh volume and "*k*" being its respective neighbor; and *n1* and *n2* represent consecutive nodes of volume "*i*", in counter-clockwise orientation.

The spatial discretization proposed by the authors is equivalent to a centered scheme with second order of accuracy, on a finite difference context. The introduction of a dissipation operator "D" is necessary to guarantee numerical stability in the presence, for example, of even-odd uncoupled solutions and nonlinear instabilities, like shock waves. So, Equation (3) is rewritten as:

$$d(V_i Q_i)/dt + \left[C(Q_i) - D(Q_i)\right] = 0. \tag{5}$$

The time integration is accomplished using a Runge-Kutta explicit method of second order and five stages and it can be represented in generalized form as:

$$\begin{aligned} Q_i^{(0)} &= Q_i^{(n)} \\ Q_i^{(k)} &= Q_i^{(0)} - \alpha_k \Delta t_i / V_i \left[C\left(Q_i^{(k-1)}\right) - D\left(Q_i^{(m)}\right)\right], \\ Q_i^{(n+1)} &= Q_i^{(k)} \end{aligned} \tag{6}$$

where $k = 1,...,5$; $m = 0$ to 4; $\alpha_1 = 1/4$, $\alpha_2 = 1/6$, $\alpha_3 = 3/8$, $\alpha_4 = 1/2$ e $\alpha_5 = 1$. The artificial dissipation operator should be evaluated only in the first two stages ($m = 0$, $k = 1$, e $m = 1$, $k = 2$), aiming CPU time economy, according to Swanson and Radespiel (1991), exploring the hyperbolic properties of the Euler equations.

3.1. Artificial dissipation operator

The artificial dissipation operator employed in this work is based on Mavriplis (1990) and can be described as:

$$D(Q_i) = d^{(2)}(Q_i) - d^{(4)}(Q_i), \tag{7}$$

where: $d^{(2)}(Q_i) = \sum_{k=1}^{3} 0{,}5\varepsilon_{i,k}^{(2)}(A_i + A_k)(Q_k - Q_i)$, named undivided Laplacian operator, is responsible to the numerical stability in the presence of shock waves; and $d^{(4)}(Q_i) = \sum_{k=1}^{3} 0{,}5\varepsilon_{i,k}^{(4)}(A_i + A_k)(\nabla^2 Q_k - \nabla^2 Q_i)$, named biharmonic operator, is responsible to the background stability (for example, even-odd instabilities). In this last term, $\nabla^2 Q_i = \sum_{k=1}^{3}(Q_k - Q_i)$. Every time that "*k*" represents a special boundary cell, named "ghost" cell, its contribution in terms of $\nabla^2 Q_k$ is extrapolated from its real neighbor volume. The ε terms are defined as:

$$\varepsilon_{i,k}^{(2)} = K^{(2)} MAX\ (\nu_i, \nu_k) \quad \text{and} \quad \varepsilon_{i,k}^{(4)} = MAX\ \left[0, \left(K^{(4)} - \varepsilon_{i,k}^{(2)}\right)\right], \tag{8}$$

where $\nu_i = \sum_{k=1}^{3} |p_k - p_i| \Big/ \sum_{k=1}^{3}(p_k + p_i)$ represents a pressure sensor. It is employed to identify regions of high gradients. $K^{(2)}$ and $K^{(4)}$ are constants and typical values are 1/4 and 3/256, respectively. Every time that "*k*" represents a ghost cell, $\nu_g = \nu_i$. The A_i terms are contributions of the maximum normal eigenvalue of the Euler equations integrated along each cell face. They are defined as:

$$A_i = \sum_{k=1}^{3}\left[\left|u_{i,k}\Delta y_{i,k} - v_{i,k}\Delta x_{i,k}\right| + a_{i,k}\left(\Delta x_{i,k}^2 + \Delta y_{i,k}^2\right)^{0,5}\right], \tag{9}$$

where $u_{i,k}$, $v_{i,k}$ and $a_{i,k}$ are calculated by arithmetical average between values of properties associated with volume "*i*" and its respective neighbor "*k*".

4. Frink, Parikh and Pirzadeh (1991) algorithm

In this scheme, the numerical flux vector is calculated using Roe (1981) flux difference splitting. The flux which crosses each cell face "*k*" is calculated using Roe formula:

$$F_k = 1/2\left[F(Q_L) + F(Q_R) - \left|\tilde{A}\right|(Q_R - Q_L)\right]_k. \tag{10}$$

In Equation (10), Q_R e Q_L are the right and the left state variables of the "*k*" flux interface, respectively. The $\tilde{A}$ matrix is determined by the evaluation of $A = \partial F/\partial Q$ with values of the flow properties obtained by Roe average:

$$\tilde{\rho} = \sqrt{\rho_L \rho_R}\ ,\ \tilde{u} = \left(u_L + u_R\sqrt{\rho_R/\rho_L}\right)\Big/\left(1 + \sqrt{\rho_R/\rho_L}\right) \quad \text{and} \quad \tilde{v} = \left(v_L + v_R\sqrt{\rho_R/\rho_L}\right)\Big/\left(1 + \sqrt{\rho_R/\rho_L}\right); \tag{11}$$

$$\tilde{h} = \left(h_L + h_R\sqrt{\rho_R/\rho_L}\right)\Big/\left(1 + \sqrt{\rho_R/\rho_L}\right) \quad \text{and} \quad \tilde{a}^2 = (\gamma - 1)\left[\tilde{h} - 0{,}5\left(\tilde{u}^2 + \tilde{v}^2\right)\right]. \tag{12}$$

It aims exactly satisfy the equality $F(Q_R) - F(Q_L) = \tilde{A}(Q_R - Q_L)$. Introducing the diagonalization matrixes $\tilde{T}$ and $\tilde{T}^{-1}$ and the diagonal matrix of eigenvalues Λ, the matrix $\left|\tilde{A}\right|$ is defined as $\left|\tilde{A}\right| = \tilde{T}\left|\tilde{\Lambda}\right|\tilde{T}^{-1}$. The term

$$\left|\tilde{A}\right|(Q_R - Q_L) = \tilde{T}\left|\tilde{\Lambda}\right|\tilde{T}^{-1}\Delta Q, \tag{13}$$

in the numerical flux vector formula of Roe, can be rewritten in terms of three flux components, each one associated with a distinct eigenvalue:

$$\tilde{T}\left|\tilde{\Lambda}\right|\tilde{T}^{-1}\Delta Q = \left|\Delta\tilde{F}_1\right| + \left|\Delta\tilde{F}_3\right| + \left|\Delta\tilde{F}_4\right|, \tag{14}$$

where:

$$\left|\Delta\widetilde{F}_1\right| = \left|\widetilde{U}\right|\left\{\left(\Delta\rho - \frac{\Delta p}{\widetilde{a}^2}\right)\begin{bmatrix} 1 \\ \widetilde{u} \\ \widetilde{v} \\ \frac{\widetilde{u}^2+\widetilde{v}^2}{2} \end{bmatrix} + \widetilde{\rho}\begin{bmatrix} 0 \\ \Delta u - n_x\Delta U \\ \Delta v - n_y\Delta U \\ \widetilde{u}\Delta u + \widetilde{v}\Delta v - \widetilde{U}\Delta U \end{bmatrix}\right\} \quad \text{and} \quad \left|\Delta\widetilde{F}_{3,4}\right| = \left|\widetilde{U} \pm \widetilde{a}\right|\left(\frac{\Delta p \pm \widetilde{\rho}\widetilde{a}\Delta U}{2\widetilde{a}^2}\right)\begin{bmatrix} 1 \\ \widetilde{u} \pm n_x\widetilde{a} \\ \widetilde{v} \pm n_y\widetilde{a} \\ \widetilde{h} \pm \widetilde{U}\widetilde{a} \end{bmatrix}, \quad (15)$$

with $\widetilde{U} = \widetilde{u}n_x + \widetilde{v}n_y$ and $\Delta U = n_x\Delta u + n_y\Delta v$.

The time integration is performed using Runge-Kutta explicit method and five stages, described by Eq. (6).

5. Spatially variable time step

A spatially variable time step, employed to each computational cell, is used with the purpose of accelerating the Jameson and Mavriplis (1986) and the Frink, Parikh and Pirzadeh (1991) schemes to the steady state solution. Details of the present implementation can be found in Maciel and Azevedo (2001) and Maciel (2002).

6. Initial and boundary conditions

6.1. Initial condition

Values of freestream flow are adopted to all properties as initial condition for this problem, in all computational domain (Jameson and Mavriplis, 1986). Therefore, the vector of conserved variables is defined as:

$$Q_i = \left\{1 \quad M_\infty \cos\alpha \quad M_\infty \sin\alpha \quad \frac{1}{\gamma(\gamma-1)} + 0{,}5M_\infty^2\right\}^t, \quad (16)$$

where M_∞ is the freestream Mach number and α is the attack angle.

6.2. Boundary conditions

The boundary conditions are basically of four types: solid wall, entrance, exit and continuity. These conditions are implemented, as commented before, in ghost cells.

(a) Wall condition: This condition imposes the flow tangency at solid wall. This condition is satisfied considering the tangent velocity component of the ghost volume at wall as equal to the respective velocity component of its real neighbor cell. At the same way, the normal velocity component of the ghost volume at wall is equal in value, but with opposite signal, to the respective velocity component of its real neighbor cell.

The normal pressure gradient of the fluid to the wall is assumed to be equal to zero according to an inviscid formulation. The same hypothesis is applied to the normal temperature gradient to the wall. From these considerations, the density and pressure of the ghost volume are extrapolated from the respective values of its real neighbor volume (zero order extrapolation). The total energy is obtained by the state equation of a perfect gas.

(b) Entrance condition:

(b.1) Subsonic flow: Three properties are specified and one extrapolated, based on information propagation analysis along characteristic directions in the calculation domain (Maciel and Azevedo, 1997, and Maciel and Azevedo, 1998). In other words, to subsonic flow, three characteristic directions of propagation information point inward to the computational domain and should be fixed. Just the characteristic direction associated to the "(q_n-a)" velocity can not be specified and should be determined by interior information from the calculation domain. The pressure was the extrapolated variable from the real neighbor volumes, for all problems studied. Density and velocity components adopted values of freestream flow. The total energy is determined by the state equation of a perfect gas.

(b.2) Supersonic flow: All variables are fixed with values of freestream flow.

(c) Exit condition:

(c.1) Subsonic flow: Three characteristic directions of propagation information point outward to the computational domain. Hence, the associated variables should be extrapolated from interior information. The characteristic direction associated to the "(q_n-a)" velocity should be specified because it point inward to the computational domain. In this case, the ghost volume pressure is specified from its initial value. Density and velocity components are extrapolated and total energy is obtained from the state equation of a perfect gas.

(c.2) Supersonic flow: All variables are extrapolated from interior domain due to all four characteristic directions of

information propagation of the Euler equations point outward to the computational domain and, therefore, nothing can be fixed.
(d) Continuity condition: Just for the physical problem of the airfoil. It is necessary that the flow continuity at the trailing edge should be satisfied (Kutta condition). This condition is assured to impose that the conserved variable vector at lower body surface should be equal to the conserved variable vector at upper body surface.

7. Results

Tests were accomplished using a CELERON-1.2GHz and 128 Mbytes of RAM memory microcomputer. Converged results occurred to a reduction of 4 orders in the value of the maximum residual. The value used to γ was 1.4. An attack angle of 0.0° was adopted for all problems.

7.1. Airfoil physical problem

A mesh of type "O" with 49x70 points or composed of 6,624 triangular volumes and 3,430 nodes was used for this problem. An exponential stretching of 5% was implemented in the normal direction in relation to body surface. The far field boundary (entrance and exit boundaries) was located at 10.0 chords in relation to airfoil's leading edge. The freestream Mach number adopted as initial condition by the simulation was 0.8, which characterizes a transonic flow. The Jameson and Mavriplis (1986) scheme reached the steady state solution in 5,422 iterations, using a CFL number of 0.5, while the Frink, Parikh and Pirzadeh (1991) scheme used a CFL number of 0.2 and the total number of iterations to obtain convergence was 8,795.

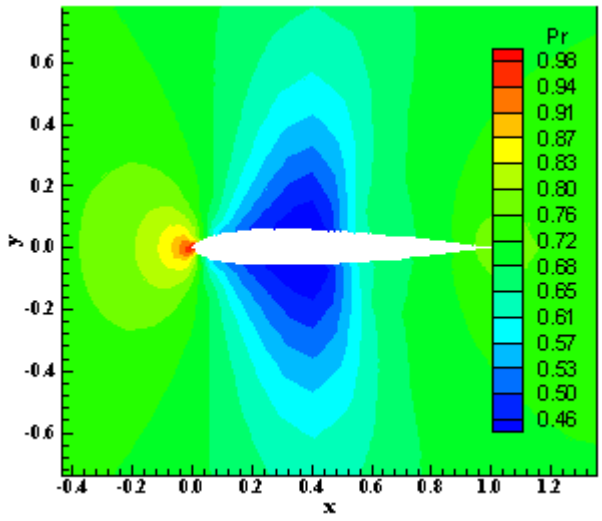

Figure 1. Pressure field (JM/86).

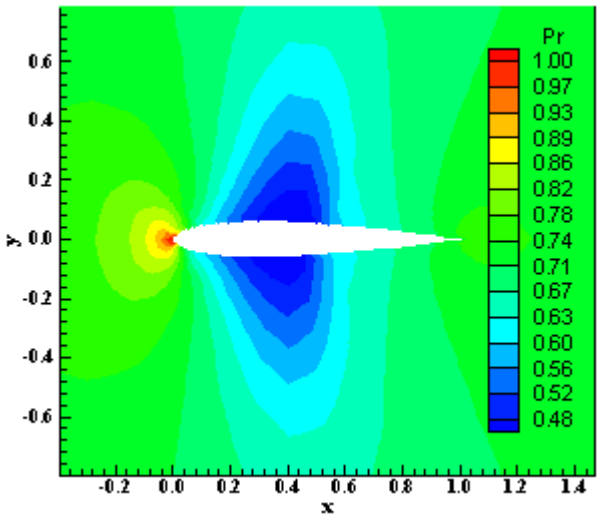

Figure 2. Pressure field (FPP/91).

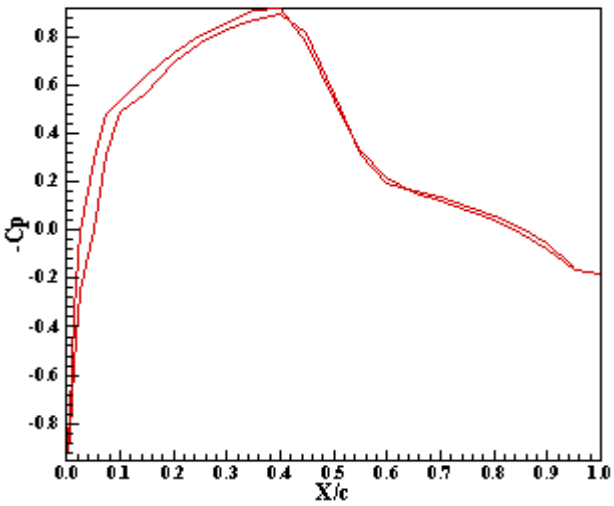

Figure 3. -Cp distribution (JM/86).

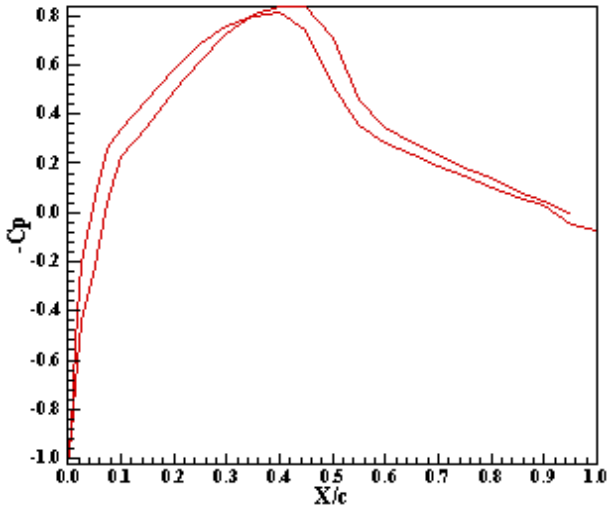

Figure 4. -Cp distribution (FPP/91).

The pressure contours obtained by both schemes do not present meaningful differences, as shows in Figs. 1 and 2, in terms of solution quality. The pressure distribution obtained by the Frink, Parikh and Pirzadeh (1991) scheme is more severe than that obtained by the Jameson and Mavriplis (1986) scheme, in quantitative terms.

The -Cp distribution, showed in Figs. 3 and 4 to both schemes, presented a shock wave acting over the airfoil. Both schemes presented this shock wave at 40% in relation to the airfoil's leading edge. The -Cp distribution obtained by the Frink, Parikh and Pirzadeh (1991) scheme is more intense than that obtained by the Jameson and Mavriplis (1986) scheme.

The computational cost of the Jameson and Mavriplis (1986) scheme was calculated in 0.0001438s/per volume/per iteration, while the computational cost of the Frink, Parikh and Pirzadeh (1991) scheme was calculated in 0.0001903s/per volume/per iteration. In other words, the Jameson and Mavriplis (1986) scheme is about 24.4% cheaper than the Frink, Parikh e Pirzadeh (1991) scheme.

7.2. VLS physical problem

An algebraic mesh of 253x70 points or composed of 34,776 triangular volumes and 17,710 nodes was used in this problem. No exponential stretching was used. The freestream Mach number adopted as initial condition was 4.0, which characterizes a supersonic flow. The Jameson and Mavriplis (1986) numerical scheme reached the steady state in 978 iterations, using a CFL number of 0.9. The Frink, Parikh and Pirzadeh (1991) scheme used a CFL number of 0.6 and the total number of iterations to obtain convergence was 3,307.

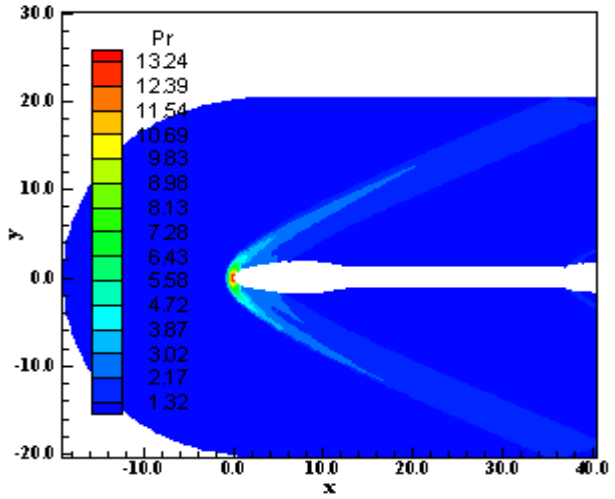

Figure 5. Pressure field (JM/86).

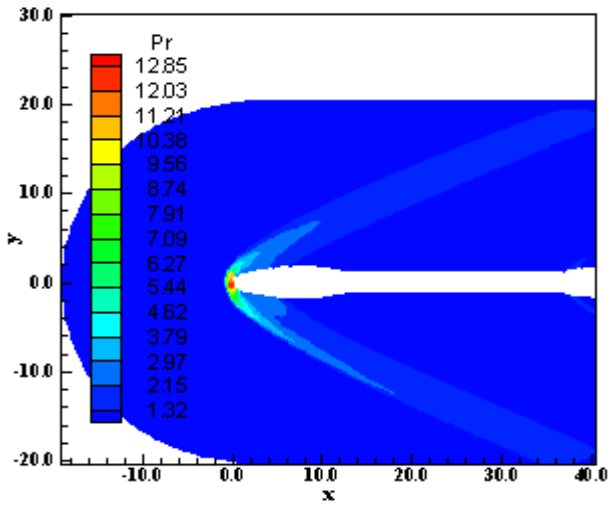

Figure 6. Pressure field (FPP/91).

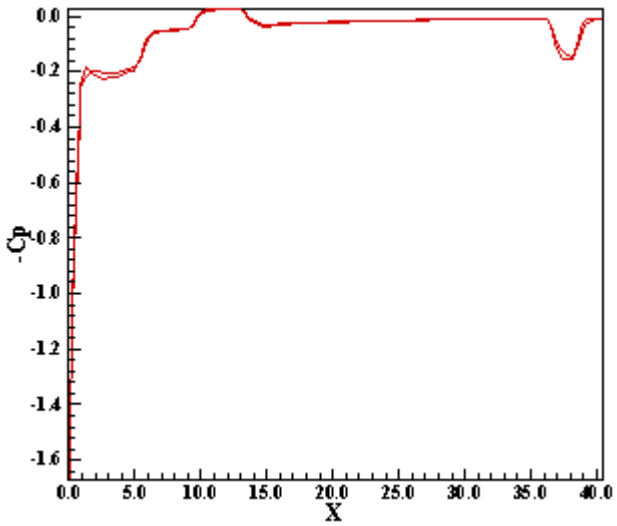

Figure 7. -Cp distribution (JM/86).

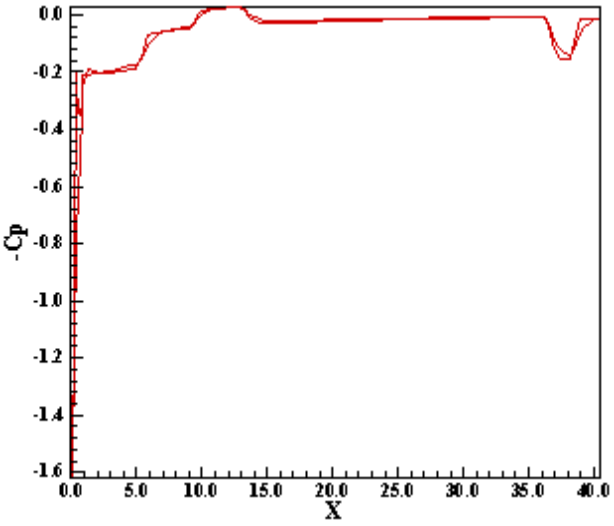

Figure 8. -Cp distribution (FPP/91).

Figures 5 and 6 show the pressure contours obtained by the Jameson and Mavriplis (1986) and the Frink, Parikh and Pirzadeh (1991) schemes. The pressure field obtained by the Jameson and Mavriplis (1986) scheme is more severe than that obtained by the Frink, Parikh and Pirzadeh (1991) scheme. Moreover, the pressure contours obtained by the Jameson and Mavriplis (1986) scheme are more symmetrical than that obtained by the Frink, Parikh and Pirzadeh (1991) scheme.

Figures 7 and 8 show the pressure distribution around the simplified version of the VLS configuration. The solutions are approximately the same, highlighting the good solution quality of the first order Frink, Parikh and Pirzadeh (1991) scheme.

8. Conclusions

This work presented the Jameson and Mavriplis (1986) and the Frink, Parikh and Pirzadeh (1991) computational characteristics. Both schemes were studied on a context of unstructured discretization of the flow equations. Both schemes were explicit and the time integration was performed using a Runge-Kutta method of five stages. The Jameson and Mavriplis (1986) scheme was second order accurate in space and the Frink, Parikh and Pirzadeh (1991) was first order accurate. A spatially variable time step was used to accelerate the convergence of the schemes to steady state condition. The transonic flow around an airfoil and the supersonic flow around a simplified version of the VLS configuration were studied.

The results presented in this work have shown that the Jameson and Mavriplis (1986) scheme has presented efficiency characteristics and solution quality better than the Frink, Parikh and Pirzadeh (1991) scheme. Although the Frink, Parikh and Pirzadeh (1991) scheme was first order accurate, good solution quality were identified in comparison with Jameson and Mavriplis (1986) scheme.

The Frink, Parikh and Pirzadeh (1991) scheme presented a computational cost about 32.3% larger than the Jameson and Mavriplis (1986) scheme, which limits its use, although, as commented before, this scheme presents good solution quality.

9. Acknowledgements

The author thanks the financial support conceded by CNPq under the form of scholarship of process number 304318/2003-5, DCR/1F.

10. References

Arnone, A., Liou, M. –S. and Povinelli, L. A., 1991, “Multigrid Calculation of Three-Dimensional Viscous Cascade Flows”, AIAA Paper 91-3238-CP.

Batina, J. T., 1990, “Unsteady Euler Airfoil Solutions Using Unstructured Dynamic Meshes”, AIAA Journal, Vol. 28, No. 8, pp. 1381-1388.

Frink, N. T., Parikh, P. and Pirzadeh, S., 1991, “Aerodynamic Analysis of Complex Configurations Using Unstructured Grids”, AIAA 91-3292-CP.

Frink, N. T., 1992, “Upwind Scheme for Solving the Euler Equations on Unstructured Tetrahedral Meshes”, AIAA Journal, Vol. 30, No. 1, pp. 70-77.

Hooker, J. R., Batina, J. T. and Williams, M. H., 1992, “Spatial and Temporal Adaptive Procedures for the Unsteady Aerodynamic Analysis of Airfoils Using Unstructured Meshes”, AIAA Paper 92-2694-CP.

Jameson, A., and Mavriplis, D. J., 1986, “Finite Volume Solution of the Two-Dimensional Euler Equations on a Regular Triangular Mesh”, AIAA Journal, Vol. 24, No. 4, pp. 611-618.

Jameson, A., Schmidt, W. and Turkel, E., 1981, “Numerical Solution of the Euler Equations by Finite Volume Methods Using Runge-Kutta Time Stepping Schemes”, AIAA Paper 81-1259.

Long, L. N., Khan, M. N. S. and Sharp, H. T., 1991, “Massively Parallel Three-Dimensional Euler / Navier-Stokes Method”, AIAA Journal, Vol. 29, No. 5, pp. 657-666.

Luo, H., Baum, J. D. and Löhner, R., 1994, “Edge-Based Finite Element Scheme for the Euler Equations”, AIAA Journal, Vol. 32, No. 6, pp. 1183-1190.

Maciel, E. S. G. and Azevedo, J. L. F., 1997, “Comparação entre Vários Algoritmos de Fatoração Aproximada na Solução das Equações de Navier-Stokes”, Proceedings of the 14th Brazilian Congress of Mechanical Engineering (also available in CD-ROM), Bauru, SP, Brazil.

Maciel, E. S. G. and Azevedo, J. L. F., 1998, “Comparação entre Vários Esquemas Implícitos de Fatoração Aproximada na Solução das Equações de Navier-Stokes”, RBCM- Journal of the Brazilian Society of Mechanical Sciences, Vol. XX, No. 3, pp. 353-380.

Maciel, E. S. G. and Azevedo, J. L. F., 2001, “Solution of Aeroespace Problems Using Structured and Unstructured Strategies”, RBCM- Journal of the Brazilian Society of Mechanical Sciences, Vol. XXIII, No. 2, pp. 155-178.

Maciel, E. S. G., 2002, “Simulação Numérica de Escoamentos Supersônicos e Hipersônicos Utilizando Técnicas de Dinâmica dos Fluidos Computacional”, Doctoral Thesis, ITA, CTA, São José dos Campos, SP, Brazil, 258 p.
Mavriplis, D. J. and Jameson, A., 1987, “Multigrid Solution of the Euler Equations on Unstructured and Adaptive Meshes”, ICASE Report No. 87-53.
Mavriplis, D. J., 1990, “Accurate Multigrid Solution of the Euler Equations on Unstructured and Adaptive Meshes”, AIAA Journal, Vol. 28, No. 2, pp. 213-221.
Roe, P. L., 1981, “Approximate Riemann Solvers, Parameter Vectors, and Difference Schemes”, Journal of Computational Physics, Vol. 43, pp. 357-372.
Swanson, R. C. and Radespiel, R., 1991, “Cell Centered and Cell Vertex Multigrid Schemes for the Navier-Stokes Equations”, AIAA Journal, Vol. 29, No. 5, pp. 697-703.

11. Responsibility notice

The author is the only responsible for the printed material included in this paper.